OPEN ACCESS
CellPress

Cell Reports
Article

GILZ Promotes Production of Peripherally Induced Treg Cells and Mediates the Crosstalk between Glucocorticoids and TGF-β Signaling

Oxana Bereshchenko,[1,2] Maddalena Coppo,[1,2] Stefano Bruscoli,[1,2] Michele Biagioli,[1] Monica Cimino,[1] Tiziana Frammartino,[1] Daniele Sorcini,[1] Alessandra Venanzi,[1] Moises Di Sante,[1] and Carlo Riccardi[1,*]
[1]Department of Medicine, Section of Pharmacology, University of Perugia, S. Andrea delle Fratte, Perugia 06132, Italy
[2]These authors contributed equally to this work
*Correspondence: carlo.riccardi@unipg.it
http://dx.doi.org/10.1016/j.celrep.2014.03.004

SUMMARY

Regulatory T (Treg) cells expressing the transcription factor forkhead box P3 (FoxP3) control immune responses and prevent autoimmunity. Treatment with glucocorticoids (GCs) has been shown to increase Treg cell frequency, but the mechanisms of their action on Treg cell induction are largely unknown. Here, we report that glucocorticoid-induced leucine zipper (GILZ), a protein induced by GCs, promotes Treg cell production. In mice, GILZ overexpression causes an increase in Treg cell number, whereas GILZ deficiency results in impaired generation of peripheral Treg cells (pTreg), associated with increased spontaneous and experimental intestinal inflammation. Mechanistically, we found that GILZ is required for GCs to cooperate with TGF-β in FoxP3 induction, while it enhances TGF-β signaling by binding to and promoting Smad2 phosphorylation and activation of FoxP3 expression. Thus, our results establish an essential GILZ-mediated link between the anti-inflammatory action of GCs and the regulation of TGF-β-dependent pTreg production.

INTRODUCTION

FoxP3$^+$ regulatory T (Treg) cells restrain the immune responses to self-antigens, pathogens, allergens, and commensal microorganisms (Feuerer et al., 2009; Josefowicz et al., 2012a). Treg cells are produced in the thymus (tTreg) but may also be generated in the periphery (pTreg) or in vitro (iTreg) by conversion of naive conventional T (Tconv) cells (Curotto de Lafaille and Lafaille, 2009; Yadav et al., 2013). Recent evidence suggests that both tTreg and pTreg cells are collectively needed to establish and maintain tolerance (Haribhai et al., 2011; Josefowicz et al., 2012b; Samstein et al., 2012). Signals required for pTreg conversion include transforming growth factor β (TGF-β), interleukin-2 (IL-2), and antigen presentation by dendritic cells. However, additional factors in tissue microenvironment, such as retinoic acid, microbiota, and its derivatives, contribute to the generation of pTreg (Atarashi et al., 2011; Coombes et al., 2007; Smith et al., 2013; Sun et al., 2007). Thus, it is important to identify factors that influence formation and maintenance of specific Treg subsets.

TGF-β signaling is a requisite for the peripheral induction of FoxP3 in naive T cells and generation of pTreg cells (Josefowicz et al., 2012a; Yadav et al., 2013). TGF-β-mediated activation of TGF-β receptors leads to phosphorylation and nuclear translocation of receptor-associated Smad proteins, leading to target gene activation (Li and Flavell, 2008). During TGF-β-mediated conversion of mature naive T cells, activated Smad2 and Smad3 bind to *foxp3* conserved enhancer region (CNS1) and cooperate with NFATc in FoxP3 induction (Takimoto et al., 2010; Tone et al., 2008). Therefore, signaling events and factors that promote or interfere with Smad phosphorylation and nuclear translocation are expected to affect Treg differentiation.

Glucocorticoid (GC) hormones are produced in adrenal glands in response to various types of stress, including inflammation (Kadmiel and Cidlowski, 2013). As potent immunosuppressors, synthetic GCs are widely used in clinics for the treatment of various autoimmune and inflammatory conditions, including inflammatory bowel diseases (IBDs) (Faubion et al., 2001). Interestingly, both in humans and mice, treatment with dexamethasone (Dex) increases the frequency of Treg cells, suggesting that GC-mediated immune suppression is in part achieved through the gain of Treg cell number or activity (Chen et al., 2006; Hu et al., 2012; Ling et al., 2007; Suárez et al., 2006). The mechanisms of GC-mediated increase in Treg frequency may involve differential sensitivity of Teff and Treg cells to GC-induced cell death (Chen et al., 2004), or facilitated generation of Treg cells upon GC stimulation (Barrat et al., 2002; Chung et al., 2004; Prado et al., 2011). To this end, GCs synergize with TGF-β signaling in FoxP3 induction (Karagiannidis et al., 2004; Prado et al., 2011). However, factors that are mediating the GC effect on FoxP3 expression and Treg cells have not been identified.

Glucocorticoid-induced leucine zipper (GILZ) was initially identified in thymocytes and peripheral T cells treated by Dex (D'Adamio et al., 1997). It is a highly responsive and predictive GC target shown to mediate several anti-inflammatory effects of GCs, including suppression of cell growth and regulation of

cell differentiation (Ayroldi et al., 2001; Bruscoli et al., 2010, 2012; Cannarile et al., 2006; Yosef et al., 2013).

Because GCs have been shown to induce Treg cells, and because GILZ is a mediator of GC effects in several contexts, we investigated the role of GILZ in Treg development and homeostasis. We report that GILZ is involved in the production of pTreg cells in vivo and that this function involves the regulation of TGF-β signaling. Moreover, GILZ is required for GC-mediated increase in Treg cells and FoxP3 expression. Thus, GILZ mediates GC-induced Treg generation by promoting TGF-β signaling.

RESULTS

GILZ Controls the Number of Treg Cells in the Periphery

To investigate the role of GILZ in GC-mediated Treg induction, as well as its physiological function in T cells, we generated mice with T cell-specific deletion of the *gilz* gene (*gilz* conditional knockout [cKO]) by breeding mice bearing the floxed *gilz* allele with CD4-Cre transgenic mice. We confirmed the absence of GILZ protein in thymocytes and in mature $CD4^+$ T cells purified from the spleens and peripheral and mesenteric lymph nodes (pLNs and mLNs, respectively) of *gilz* cKO mice (Figure S1A).

Mice lacking GILZ in T cells showed normal frequencies and the number of $CD4^-CD8^-$ double-negative, $CD4^+CD8^+$ double-positive, and $CD4^+/CD8^+$ single-positive (SP) T cell subpopulations in thymus and peripheral lymphoid organs (Figure S1B). These data demonstrated that GILZ is dispensable for normal T cell development and formation of $CD4^+$ and $CD8^+$ cells.

We next tested whether GILZ, as an effector of GCs, regulates the production of Treg cells in vivo. *gilz* cKO mice showed similar frequency and the absolute number of $CD4^+FoxP3^+$ tTreg cells compared to their littermate controls (Figures 1A–1C). Because tTreg cells were still formed in the absence of GILZ, we concluded that GILZ was not essential for the development of $FoxP3^+$ cells in the thymus.

To the contrary, the frequency and the absolute number of $CD4^+FoxP3^+$ cells found in spleens (Figures 1D and 1E) and mLNs (Figures 1G and 1H) of 9- to 11-week-old mice were moderately but significantly diminished in *gilz* cKO mice compared to controls, despite similar total number of cells (Figures 1F and 1I), and $CD4^+$ cells were present in the respective organs (Figure S1B). GILZ-deficient mice also did not support an age-dependent increase in the frequency of $FoxP3^+$ cells because a smaller proportion of $CD4^+$ T cells expressed FoxP3 in the spleens of 12-month-old *gilz* cKO mice (Figure 1J).

As a complement to the gene deletion approach, we also addressed the effect of GILZ overexpression on Treg cell formation in mice constitutively overexpressing GILZ in T cell lineage (*gilz* TG) (Delfino et al., 2004). Forced expression of GILZ caused an increase in the frequency and the absolute number of $CD4^+FoxP3^+$ cells in spleens (Figures 1K and 1L) and mLNs (Figures 1M and 1N), without affecting the number of CD4 and CD8 SP cells (Figures S1C and S1D). Collectively, these data demonstrate that GILZ positively regulates the number of Treg cells in the periphery.

GILZ Is Required for pTreg Cell Formation

The decrease in Treg cell number was not associated with the reduced capacity of GILZ-deficient cells to cycle in vivo (Fisson et al., 2003), as measured by the expression of the proliferation marker Ki67 (Figure S2A). GILZ-deficient $CD4^+CD25^+$ cells also did not reveal evidence of decreased survival because we detected similar rates of spontaneous apoptosis in vitro (Figure S2B), caspase activity (Figure S2C), and the expression of pro- and antiapoptotic genes of the *bcl2* family (Figure S2D). The Treg reduction could also not be ascribed to a reduced production of TGF-β or IL-2 because GILZ-deficient $CD4^+CD25^-$ cells produced similar levels of *Tgfb1* and *Il2* mRNA (Figures S2E and S2F). To further demonstrate that the decrease in the peripheral Treg cell number in *gilz* cKO mice was not due to their reduced maintenance in vivo, we have intravenously (i.v.) injected carboxyfluorescein succinimidyl ester (CFSE)-labeled lymphocytes isolated from the spleens and pLNs of wild-type (WT) and *gilz* cKO mice ($CD45.2^+$ allotype) into unmanipulated congenic hosts ($CD45.1^+$ allotype) and followed the survival and proliferation of donor-derived cells over time. The number of *gilz* cKO $CD45.2^+CD4^+FoxP3^+$ (Figure S2G, left) and $CD45.2^+CD4^+FoxP3^-$ cells (Figure S2G, right) did not significantly differ from that of donor-derived WT cells. This is in agreement with a similar frequency of WT and *gilz* cKO $CD4^+FoxP3^+$ cells that have divided in vivo, as detected by dilution of the CFSE dye (Figure S2H).

Normal tTreg frequencies and a relatively small decrease in Treg cell number in the periphery point to the possibility that GILZ regulates the generation of pTreg cells that constitute less than 20% of peripheral Treg pool size in C57Bl/6 mice (Weiss et al., 2012; Yadav et al., 2012). Naive GILZ-deficient $CD4^+$ T cells showed impaired induction of FoxP3 in vitro, compared to similarly treated WT cells (Figure 2A). The defect was specific to iTreg differentiation because naive *gilz* cKO T cells efficiently upregulated the mRNA expression of Th1, Th2, and Th17 master regulators under relative polarizing conditions (Figure 2B). To test whether GILZ regulates pTreg cell generation in vivo, we have evaluated conversion of naive $CD4^+CD25^-CD45Rb^{hi}$ T cells from WT and *gilz* cKO mice upon transfer into $RAG1^{-/-}$ mice. We found that about 2.5% of WT Tconv cells isolated from the mLNs of recipient mice had differentiated into $FoxP3^+$ pTreg cells. In contrast, significantly fewer GILZ-deficient T cells became $FoxP3^+$ (Figure 2C). The difference in conversion between WT and GILZ-deficient cells was stronger evidenced in colon lamina propria (LP) because less than 1% (4-fold decrease) of $CD4^+$ T cells isolated from colon LP of mice transferred with GILZ-deficient Tconv cells expressed FoxP3 (Figure 2D). These results demonstrate that Tconv cells lacking GILZ were defective in converting into Treg cells both in vitro and in vivo.

pTreg cells generated in a tolerogenic environment are largely $Nrp\text{-}1^-$ (Weiss et al., 2012; Yadav et al., 2012). We thus have used the expression of Nrp-1 to distinguish tTreg and pTreg cells and to test whether the Treg decrease in *gilz* cKO mice derives from a selective loss of pTreg cells. We have found that *gilz* cKO mice have a significant decrease in the frequency (Figures 2E and 2F) and the number of $CD4^+FoxP3^+Nrp\text{-}1^-$ pTreg cells (Figures 2G and 2H, left), whereas the absolute number of $CD4^+FoxP3^+Nrp\text{-}1^+$ tTreg cells did not differ (Figures 2G and 2H, right). Consistent with the idea that GILZ regulates pTreg production, the frequency and the number of $CD4^+FoxP3^+$ cells

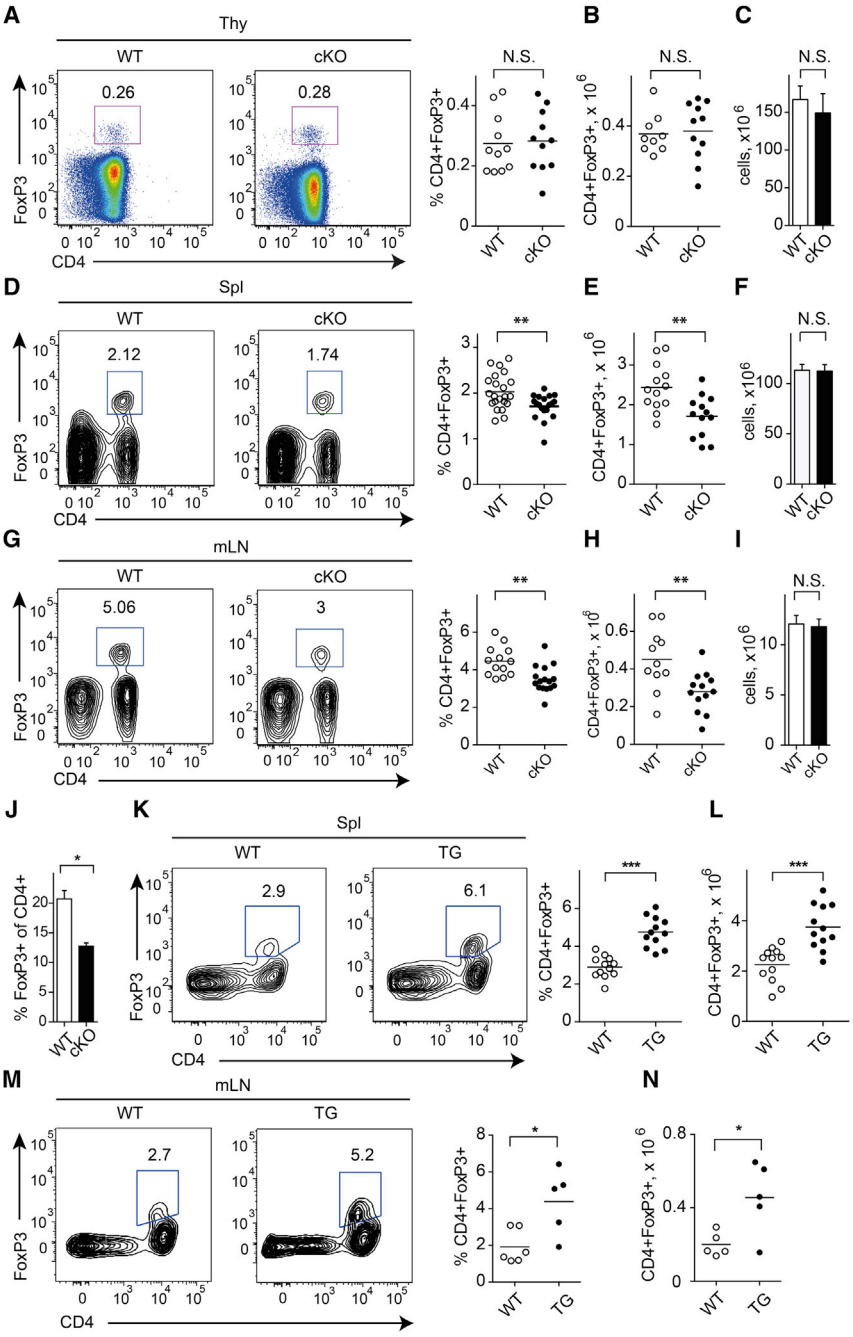

Figure 1. GILZ Controls the Number of Treg Cells in the Periphery

(A) Flow cytometry analysis of CD4 and FoxP3 expression in thymi of 9- to 11-week-old WT and *gilz* cKO mice. N.S., not significant.

(B) Number of $CD4^+FoxP3^+$ cells in thymi of 9- to 11-week-old WT and *gilz* cKO mice.

(C) Number of cells in thymi of 9- to 11-week-old WT and *gilz* cKO mice (n = 10/group).

(D and E) Frequency (D) and number (E) of $CD4^+FoxP3^+$ cells in spleens of 9- to 11-week-old WT and *gilz* cKO mice.

(F) Number of cells in spleens of 8- to 12-week-old WT and *gilz* cKO mice (n = 20/group).

(G and H) Frequency (G) and number (H) of $CD4^+FoxP3^+$ cells in mLNs isolated from 8- to 11-week-old WT and *gilz* cKO mice.

(I) Number of cells in mLNs of 8- to 12-week-old WT and *gilz* cKO mice (n = 10/group).

(J) Frequency of $FoxP3^+$ cells among $CD4^+$ cells in spleens of 12-month-old WT and *gilz* cKO mice (n = 5/group).

(K and L) Frequency (K) and number (L) of $CD4^+FoxP3^+$ cells in spleens of 12- to 13-week-old WT and *gilz* TG mice.

(M and N) Frequency (M) and number (N) of $CD4^+FoxP3^+$ cells in mLNs of 12- to 13-week-old WT and *gilz* TG mice.

Numbers close to the gates show the frequency of the gated population. Each symbol represents an individual mouse; small horizontal lines indicate the mean (A–L). Graphs represent mean ± SEM. Data are from one (M and N), or a pool of two (K and L), three (A–C and G–H), or six (D–F) independent experiments. See also Figure S1.

were strongly downregulated in the colon of *gilz* cKO mice (Figures 2I–2K). Altogether, our data suggest that the absence of GILZ selectively affects generation of pTreg cells in the periphery.

Analysis of GILZ expression in $CD4^+CD25^-$ and $CD4^+CD25^+$ purified from WT mice shows that both GILZ mRNA and protein were found at higher levels in $CD4^+CD25^-$ T cells than in $CD4^+CD25^+$ Treg-enriched cells (Figures S3A and S3B). This suggests that GILZ is required in Tconv cells for efficient Treg conversion and suggests that it might be dispensable for the Treg function, once they are formed. Consistent with this idea, we have not found differences in the expression of Treg-associated markers such as CD25, GITR, and CTLA-4, as well as activation markers such as CD69 and CD103 between WT and GILZ-deficient $CD4^+FoxP3^+$ cells (Figure S3C). Because the expression of FoxP3 closely correlated with CD25 expression in *gilz* cKO mice as it is observed in WT mice (data not shown), we used CD25 expression to purify Treg cells for functional studies. Cotransfer of an equal number of WT and GILZ-deficient $CD4^+CD25^+$ cells with naive colitogenic WT $CD4^+CD25^-CD45Rb^{hi}$ cells into immunodeficient hosts (Powrie et al., 1993) revealed a similar capacity of GILZ-deficient Treg cells to suppress effector cell expansion and body weight loss caused by Tconv-mediated colitis to the one of the WT $CD4^+CD25^+$ cells (Figures S3D and S3E). In agreement with the unimpaired in vivo suppressor function of GILZ-deficient Treg cells, we found similar amounts of transcript and per-cell protein levels of FoxP3 (Figures S3F and S3G). Taken together, these data suggest that GILZ is expressed and is required in Tconv cells for pTreg conversion and is dispensable in Treg suppressive function.

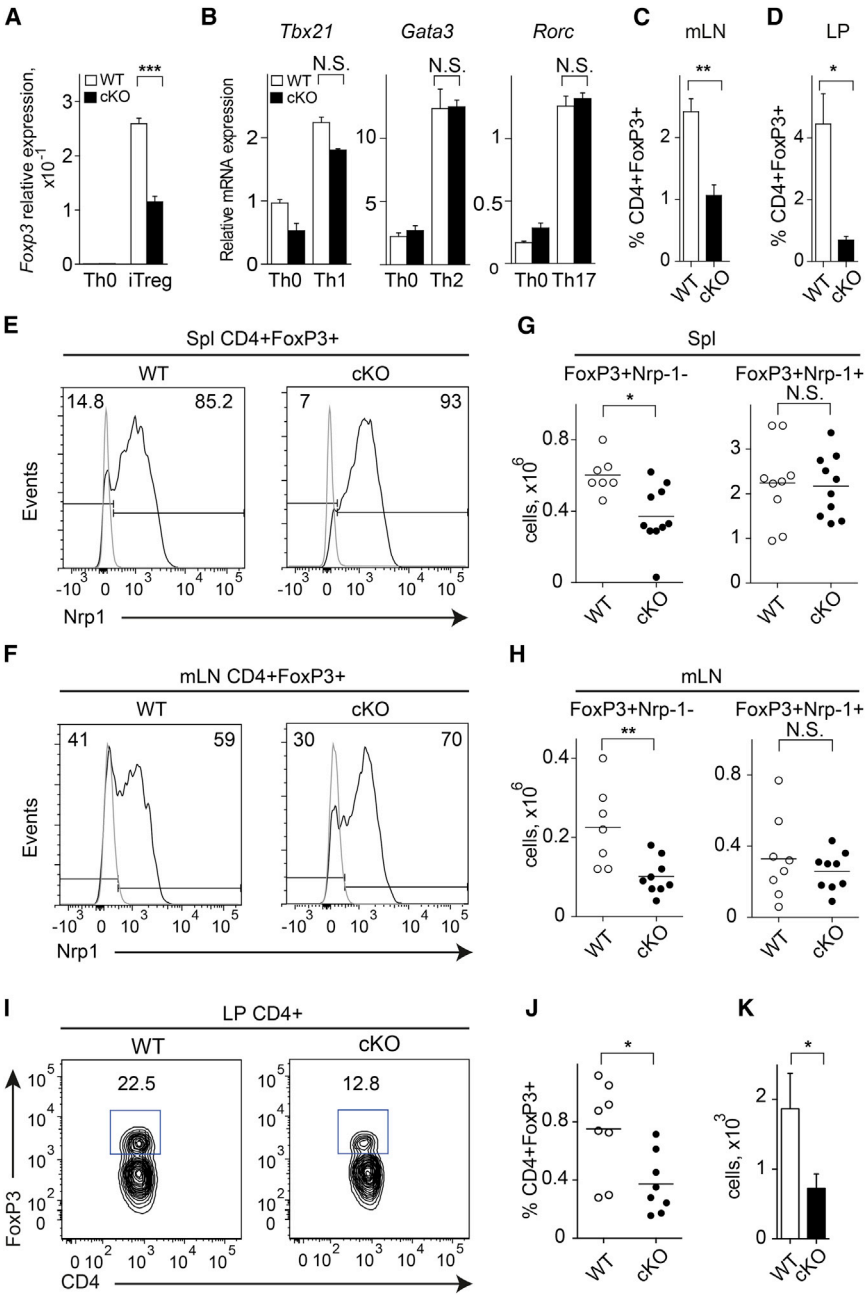

Figure 2. GILZ Is Required for pTreg Cell Formation

(A) Quantitative real-time PCR analysis of *Foxp3* mRNA expression in sorted naive $CD4^+CD62L^{hi}CD44^{lo}CD25^-$ T cells differentiated for 48 hr in Th0 and iTreg conditions (as described in the Experimental Procedures).

(B) Quantitative real-time PCR analysis of *Tbx21*, *Gata3*, and *Rorc* mRNA expression in naive T cells differentiated for 48 hr in Th1, Th2, and Th17 conditions. Data in (A) and (B) are presented relative to the expression of *Actb* mRNA.

(C and D) Frequency of $CD4^+FoxP3^+$ cells in mLNs (C) and LP (D) of $Rag1^{-/-}$ mice at 6 weeks following the adoptive transfer of $CD4^+CD25^-CD45RB^{hi}$ cells isolated from WT and *gilz* cKO mice (n = 5–6/group).

(E and F) Flow cytometry analysis of Npr-1 expression on $CD4^+FoxP3^+$ cells in spleens (E) and mLNs (F) of 11- to 20-week-old WT and *gilz* cKO mice. Gray lines show fluorescence-minus-one (FMO) controls for Nrp-1 staining.

(G and H) Number of $FoxP3^+Nrp\text{-}1^-$ (left) and $FoxP3^+Nrp\text{-}1^+$ (right) cells in spleens (G) and mLNs (H) of WT and *gilz* cKO mice.

(I) Frequency of $FoxP3^+$ cells among $CD4^+$ cells in colon LP of 10- to 12-week-old WT and *gilz* cKO mice (n = 5/group).

(J and K) Frequency and number of $CD4^+FoxP3^+$ cells in colon LP of 12- to 20-week-old WT and *gilz* cKO mice.

Graphs represent mean ± SEM. Data are representative of three (A and B) or a pool of two (C and D) or three (E–K) independent experiments.

See also Figure S2.

Loss of Immune Homeostasis in Aged *gilz* cKO Mice

Deletion of GILZ did not result in general T cell activation and overt inflammation (data not shown). Nevertheless, over time, *gilz* cKO mice developed spontaneous colon inflammation, as evidenced by a moderate increase in colonic LP lymphocytes (Figure 3A) and colon weight-to-length ratio (Figure 3B) observed in 12-month-old *gilz* cKO mice. This was associated with the decrease in the frequency and the absolute number of $CD4^+FoxP3^+$ cells in the colons of aged *gilz* cKO mice compared to their WT controls (data not shown).

The infiltrating leukocytes produced more *Ifng* but not *Il4* and *Il17* mRNA (data not shown), whereas mLN cells (Figure 3C) and LP $CD4^+$ T cells (Figure 3D) produced more interferon (IFN)-γ, but not IL-4 and IL-17 cytokines, suggesting that a decrease in Treg cell number is associated with the loss of intestinal immune homeostasis in aging *gilz* cKO mice.

Because in the *gilz* cKO mice, GILZ is missing in all T cells, including Tconv cells, we cannot exclude that the spontaneous colon inflammation develops due to a self-intrinsic effect in Teff cells, rather than to a reduced tolerance. $CD4^+FoxP3^-$ Tconv and $CD8^+$ cells isolated from 8- to 11-week-old WT and *gilz* cKO mice showed similar activation and proliferation states, as analyzed by the expression of CD62L, CD44, and Ki67 markers (Figures 3E and 3F). To directly address the effector function of Tconv cells, we compared the ability of WT and GILZ-deficient Tconv cells to induce colitis in vivo. Transfer of naive $CD4^+CD25^-CD45Rb^{hi}$ T cells sorted from *gilz* cKO mice caused a similar degree of body weight loss and clinical signs of colitis as the one caused by the transfer of WT cells (Figure 3G). Consistent with similar colitogenic activity, transferred WT and GILZ-deficient $CD4^+FoxP3^-$ T cells proliferated equally in the mLNs of $Rag1^{-/-}$ animals (Figure 3H) and were present at similar

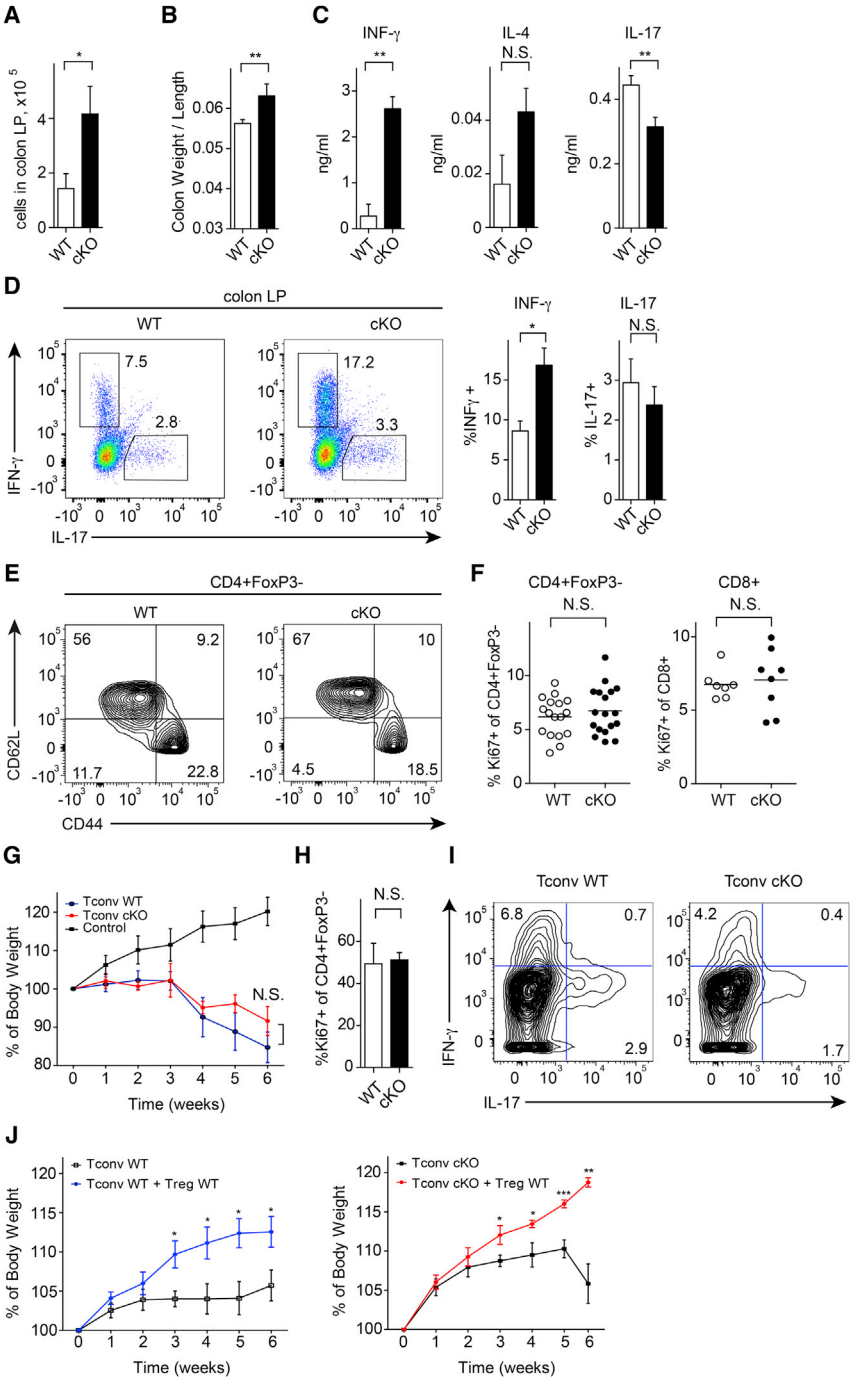

Figure 3. Loss of Immune Homeostasis in Aged *gilz* cKO Mice

(A) Total number of lymphocytes isolated from colon LP of 12-month-old WT and *gilz* cKO mice (n = 11/group).

(B) Weight-to-length ratio of the colons of 12-month-old WT and *gilz* cKO mice (n = 7–18/group).

(C) ELISA of IFN-γ, IL-4, and IL-17 expression in mLNs of aged (>12 months old) WT and *gilz* cKO mice (n = 6–8/group).

(D) Intracellular flow cytometry analysis of IFN-γ and IL-17 expression by $CD4^+$ cells isolated from colon LP of aged WT and *gilz* cKO mice (n = 4/group).

(E) Flow cytometry analysis of CD62L and CD44 in $CD4^+FoxP3^-$ cells in spleens of 9- to 11-week-old WT and *gilz* cKO mice (n = 8/group).

(F) Frequency of $Ki67^+$ cells among $CD4^+FoxP3^-$ and $CD8^+$ cells in spleens of 9- to 11-week-old WT and *gilz* cKO mice.

(G) Change in body weight of $Rag1^{-/-}$ mice that received WT or *gilz* cKO $CD4^+CD25^-CD45RB^{hi}$ cells, compared to control mice injected with PBS (mean ± SD; n = 10/group).

(H) Frequency of $Ki67^+$ cells among $CD4^+FoxP3^-$ cells in mLNs of $Rag1^{-/-}$ mice injected as in (F), isolated 6 weeks after cell transfer (n = 4–6/group).

(I) Flow cytometry analysis of the IFN-γ and IL-17 expression by mLNs isolated from $Rag1^{-/-}$ mice injected as in (G), 6 weeks after cell transfer. Plots are representative of four to five mice per group.

(J) Change in body weight of $Rag1^{-/-}$ mice following the adoptive transfer of $CD4^+CD25^-CD45RB^{hi}$ from WT (left) or *gilz* cKO (right) donors transferred alone or together with $CD4^+CD25^+$ T cells sorted from WT donors (n = 7–9/group).

Graphs represent mean ± SEM. Data are from one (J), two (C, D, and I), or a pool of three (A–H) or six (E, left) experiments. See also Figure S3.

numbers in the spleen and mLN (data not shown). Importantly, GILZ-deficient Teff cells did not produce more IFN-γ and IL-17 cytokines compared to WT cells (Figure 3I). Finally, the colitogenic WT and *gilz* cKO cells were equally responsive to Treg-mediated suppression because cotransfer of WT $CD4^+CD25^+$ cells significantly reversed the body weight loss caused by both WT and *gilz* cKO $CD4^+CD25^-CD45Rb^{hi}$ cells (Figure 3J). Taken together, these data indicate that GILZ deficiency affects Treg development and consistently leads to Th1-type spontaneous tissue inflammation with age.

Lack of GILZ in T Cells Exacerbates Chemically Induced Colitis

Because deregulated Teff and Treg cell responses are implicated in the pathogenesis of IBD, and because aging *gilz* cKO mice appear to be predisposed to the development of colitis, we tested whether GILZ deficiency influences the susceptibility to experimentally induced colitis (Cannarile et al., 2009). The severity of dinitrobenzene sulfonic acid (DNBS)-induced colitis, as measured by body weight loss, diarrhea scoring, and colon shortening, was markedly increased in *gilz* cKO mice compared to similarly treated WT controls (Figures 4A–4C). The calculated colon weight-to-length ratio, histologic damage, and total clinical score were elevated in DNBS-treated *gilz* cKO mice, compared to WT mice (Figures 4D–4F). An augmented degree of intestinal inflammation was also evidenced by the increased levels of *Tnfa*

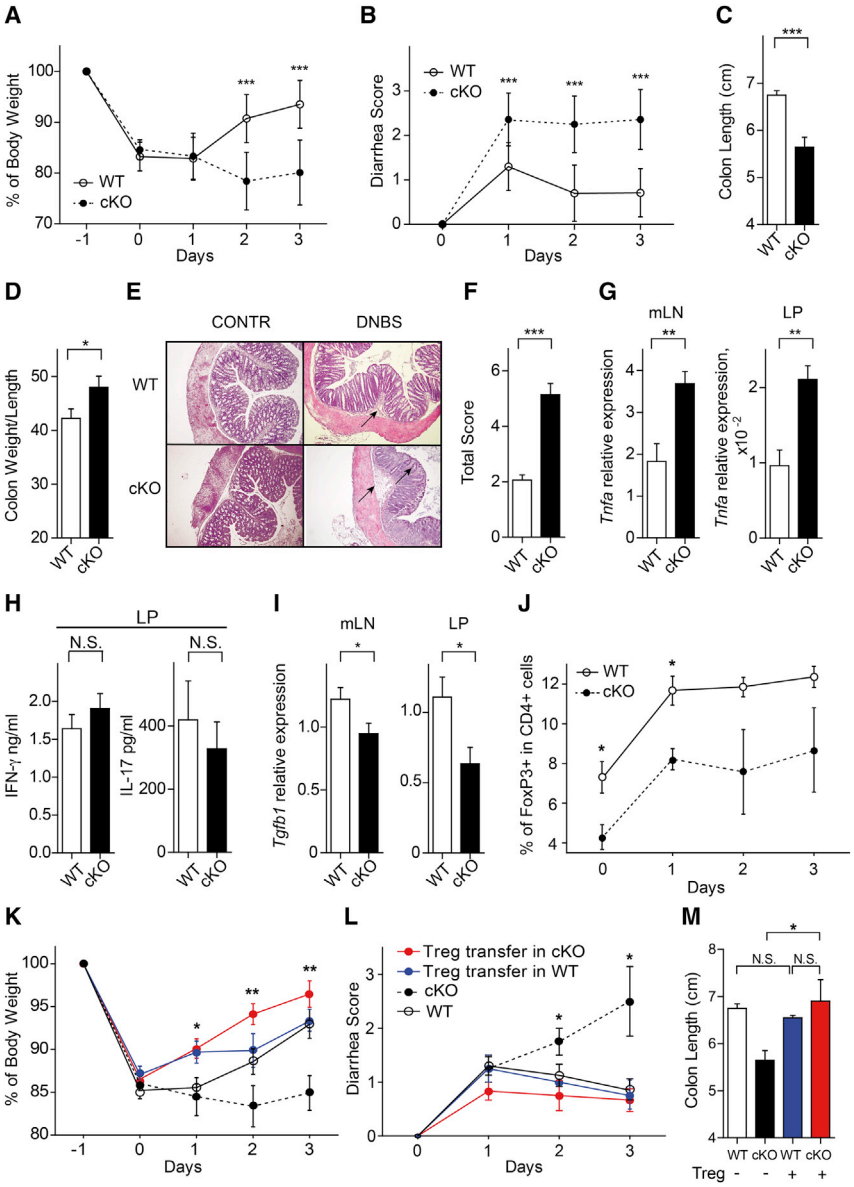

Figure 4. Lack of GILZ in T Cells Exacerbates Chemically Induced Colitis

(A) Changes in body weight of WT and *gilz* cKO mice during the course of DNBS-induced colitis. Mice were put on a diet on day −1, and DNBS was administered at Day 0.

(B) Diarrhea score of WT and *gilz* cKO mice at 3 consecutive days following DNBS administration (mean ± SD; n = 12–13/group).

(C) Colon length of WT and *gilz* cKO mice at day 3 after DNBS administration.

(D) Ratio between colon weight and colon length in WT and *gilz* cKO mice with DNBS-induced colitis.

(E) Histology of the colon in control and DNBS-treated WT and *gilz* cKO mice. Arrows indicate signs of morphological damage and/or leukocytes infiltration.

(F) Total colitis score in WT and *gilz* cKO mice with DNBS-induced colitis at day 3 after DNBS administration (n = 7–8/group).

(G) Quantitative real-time PCR analysis of *Tnfa* mRNA expression in mLN cells (left) and in colon LP lymphocytes (right), presented relative to the expression of *Actb* mRNA (n = 7–8/group).

(H) ELISA of INF-γ (left) and IL-17 (right) in supernatants of lymphocytes isolated from colon LP of WT and *gilz* cKO mice at day 3 after DNBS administration and cultured with plate bound anti-CD3 and anti-CD28 Abs for 48 hr (n = 3/group).

(I) Quantitative real-time PCR analysis of *Tgfb1* expression in mLNs and in LP, presented relative to the expression of *Actb* mRNA (n = 7–8/group).

(J) Number of $FoxP3^{+}CD4^{+}$ cells in mLNs isolated from WT and *gilz* cKO mice at day 3 after DNBS administration (n = 4/group).

(K and L) Changes in body weight (K) and diarrhea score (L) of WT and *gilz* cKO mice during the course of DNBS-induced colitis with or without pretransfer of WT $CD4^{+}CD25^{+}$ cells (Treg).

(M) Colon length of WT and *gilz* cKO mice at day 3 after DNBS administration, with or without Treg transfer.

Graphs represent mean ± SEM. Data are pooled from two (G and I–M) or five (A–F) experiments or from one of two experiments with similar results (H). See also Figure S4.

transcripts in mLNs and the colon LP of DNBS-treated *gilz* cKO mice, compared to similarly treated WT controls (Figure 4G). Of note, we did not detect elevated production of IL-17 and IFN-γ by lymphocytes isolated from the colon LP of DNBS-treated *gilz* cKO mice (Figure 4H). Lower expression of *Tgfb1* mRNA in mLNs and LP pointed to attenuated suppressive responses in GILZ-deficient mice (Figure 4I). Consistently, we have found a reduced frequency of $FoxP3^{+}$ cells in mLNs of *gilz* cKO mice during the first 3 days of colitis (Figure 4J), whereas the frequency of $FoxP3^{-}IL\text{-}10^{+}$ cells and overall production of IL-10 did not seem to vary (data not shown). Importantly, the pretransfer of WT Treg cells reversed the increased susceptibility to DNBS into *gilz* cKO mice (Figures 4K–4M). Moreover, we have also observed that *gilz* cKO mice are more susceptible to oxazolone-induced colitis (Th2 type), suggesting that pTreg deficiency observed in these mice may also favor Th2-type intestinal inflammation (Figure S4). Taken together, these results demonstrate that *gilz* cKO mice develop stronger intestinal inflammation in response to chemically induced tissue damage, a phenotype associated with reduced Treg cell number.

GILZ Deficiency Precludes Dex-Mediated Alleviation of DNBS-Induced Colitis, Induction of Treg Cells, and Cooperation with TGF-β in FoxP3 Induction

GC treatment is extensively used in IBD therapy. We tested for GILZ's requirement for the responsiveness of DNBS-treated mice to Dex treatment. Figure 5 shows that three daily injections with Dex (1.5 mg/kg) accelerated the body weight recovery and improved diarrhea score and overall clinical and histologic score in DNBS-treated WT mice. Because one of the many

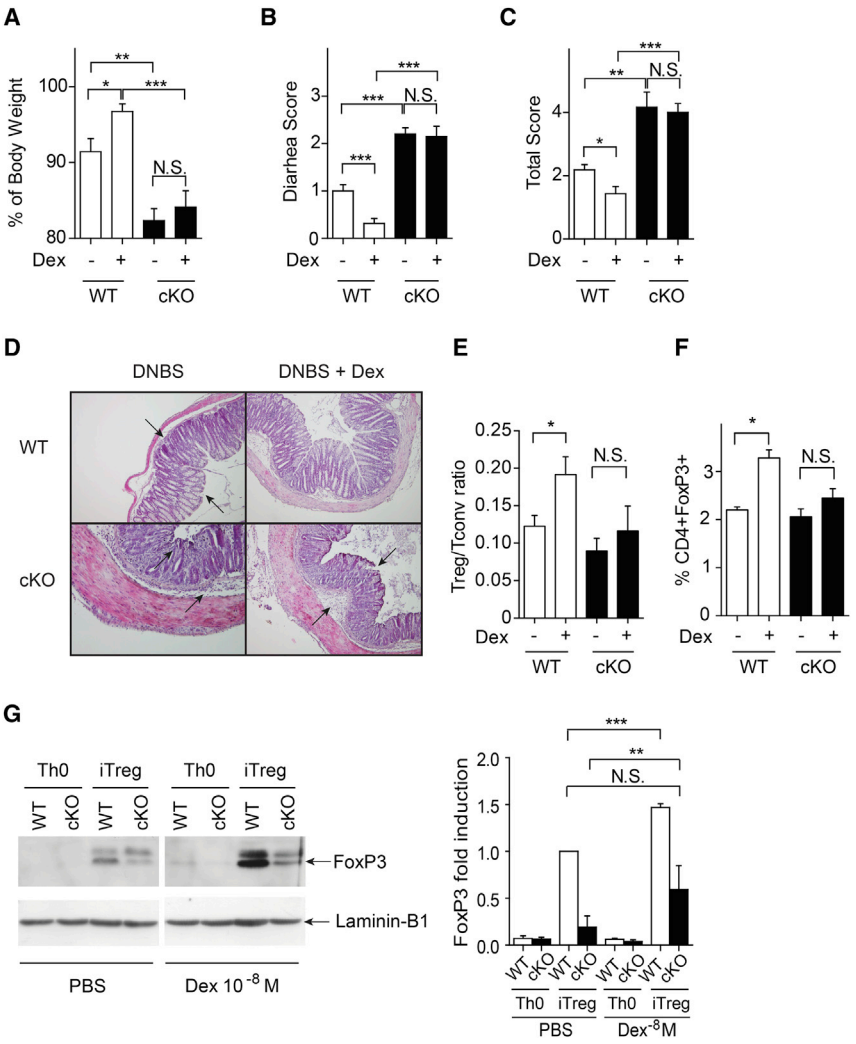

Figure 5. GILZ Deficiency Precludes Dex-Mediated Alleviation of DNBS-Induced Colitis, Induction of Treg Cells, and Cooperation with TGF-β in FoxP3 Induction

(A) Percentage of body weight of WT and *gilz* cKO mice at day 3 after DNBS administration at day 0 and daily i.p. treatment with Dex (1.5 mg/kg) relative to initial body weight. Control mice were treated with PBS.

(B) Diarrhea score of WT and *gilz* cKO mice treated as in (A).

(C) Total clinical score in WT and *gilz* cKO mice treated as in (A) (n = 12–13/group).

(D) H&E-stained histologic slides from distal colon sections (10×) of WT and *gilz* cKO mice treated as in (A). Arrows indicate signs of morphological damage and/or leukocytes infiltration.

(E) Ratio between Treg and Tconv cell frequencies in colons of WT and *gilz* cKO mice treated as in (A) (n = 3–5/group).

(F) Frequency of $CD4^+FoxP3^+$ cells in spleens isolated from WT and *gilz* cKO mice treated for 3 consecutive days with Dex (1 mg/kg) (n = 3–5/group).

(G) WB analysis of FoxP3 expression in $CD4^+CD25^-$ cells isolated from WT and *gilz* cKO mice, pretreated with Dex (10^{-8}M) for 24 hr in the presence of plate bound anti-CD3 and anti-CD28 Abs and then cultured for 48 hr in Th0 and iTreg conditions. Same number of cells was loaded; WB with anti-Laminin-B1 antibodies served as loading control. Graph to the right shows densitometry analysis of FoxP3 expression.

Graphs represent mean ± SEM. Data are a pool of five (A–C) or two (G) experiments, or from one of three independent experiments with similar results (E and F). See also Figure S5.

anti-inflammatory effects of GCs is the increase of the Treg cell frequency, we have analyzed and found the increase in the Treg-to-Tconv cell ratio in the colons of WT mice (Figure 5E), suggesting that modulation of Treg cell number in colon LP contributes to the therapeutic effects of Dex. Of note, Dex treatment did not change the Treg/Tconv ratio in *gilz* cKO mice, did not promote body weight recovery, and did not alleviate the colitis scores (Figures 5A–5E), thus showing that a lack of GILZ precludes GC-mediated anti-inflammatory effects during colitis treatment, which is associated with a GILZ-dependent increase of Treg-to-Teff cell ratio.

We next tested whether GCs require GILZ to increase the Treg cell frequency also in unmanipulated mice (Chen et al., 2004). As expected, injection with Dex for 3 consecutive days augmented the frequency of splenic $CD4^+FoxP3^+$ cells in 6- to 8-week-old WT mice (that at this age are not yet revealing significant differences in Treg cell number), but it failed to do so in mice lacking GILZ (Figure 5F). These results demonstrate that GILZ is at least partially responsible for the GC-mediated effect on Treg cells.

We then tested whether GCs were able to augment TGF-β-induced FoxP3 expression in the absence of GILZ (Prado et al., 2011). $CD4^+CD25^-$ T cells purified from WT and *gilz* cKO mice were activated for 24 hr in the presence of 10^{-8}M Dex and then stimulated with TGF-β to induce iTreg cell differentiation. Pretreatment with Dex strongly increased the TGF-β-induced FoxP3 expression in WT, but not in GILZ-deficient, cells (Figure 5G). Thus, GCs cooperate with TGF-β in FoxP3 induction and Treg differentiation in a GILZ-dependent manner.

Because phosphorylated Smad proteins are critical effectors of TGF-β signaling in T cells, we next tested whether Dex enhanced the TGF-β-induced phosphorylation of Smad2 (p-Smad2). Figure S5A (top panel) shows that Dex resulted in about a 2-fold increase in p-Smad2-to-total Smad2 protein level ratio. Dex treatment alone did not significantly induce p-Smad2, suggesting that Dex synergizes with TGF-β to induce p-Smad2 and FoxP3 expression. This idea is further supported by the fact that the activity of TGF-β receptor I (TGF-βRI) was required for the effect of Dex because Dex-pretreated cells that were also treated with the selective inhibitor of TGF-βRI (SB 431542) were not able to upregulate p-Smad2 (Figure S5B, top panel) and, consequently, *foxp3* mRNA (Figure S5C), upon stimulation with

TGF-β. Similar data were obtained using another TGF-βRI inhibitor, GW788388 (data not shown). We therefore conclude that Dex synergizes with TGF-β in FoxP3 expression, and the synergy involves modulation of GILZ expression and p-Smad2.

GILZ Enhances TGF-β Signaling and FoxP3 Expression via Direct Stimulation of TGF-β Signaling

To dissect the mechanism of GILZ's effect on TGF-β signaling, we tested the levels of p-Smad2 in WT and GILZ-deficient $CD4^+CD25^-$ T cells treated in vitro with TGF-β. GILZ-deficient cells showed comparable levels of total Smad2 protein as WT cells but reduced TGF-β-induced p-Smad2 (Figure 6A), suggesting that TGF-β-induced signaling cascade is defective in T cells lacking GILZ.

To test whether GILZ interacts with TGF-β downstream signaling components, we first performed transient overexpression coimmunoprecipitation experiments in 293T cells. The results show that GILZ interacts with Flag-tagged Smad2 and Smad4 (Figures 6B and 6C), but not with Smad3 (Figure S6). The binding between Smad proteins and GILZ is direct as shown in glutathione S-transferase (GST) pull-down experiments using GST-Tat-GILZ and Flag-Smad2/Smad4 purified from bacterial extracts (Figure 6D). Importantly, we show that the interaction between GILZ and Smad2 occurs physiologically in native $CD4^+CD25^-$ T cells upon stimulation with TGF-β (Figure 6E).

Smad2 and Smad3 are collectively essential for the activation of the FoxP3 expression during iTreg cell conversion via their direct binding to a *foxp3* CNS1 (Takimoto et al., 2010; Tone et al., 2008). To test whether the attenuated Smad phosphorylation observed in GILZ-deficient T cells results in their compromised transcriptional activity, we performed chromatin immunoprecipitation (ChIP) assays using $CD4^+CD25^-$ T cells purified from WT and *gilz* cKO mice and activated in vitro in the presence of TGF-β. TGF-β induced Smad2 binding to CNS1 (Figure 6F, left) and consequent acetylation of histone H3 (Figure 6F, right) only in GILZ-sufficient cells. Consistently, levels of FoxP3 protein expression, which was subsequently induced in WT cells, were greatly reduced in cells lacking GILZ (Figure 6G). Importantly, we were able to restore the *foxp3* mRNA expression in GILZ-deficient $CD4^+CD25^-$ cells, transfected with Smad2 expression vector and stimulated with TGF-β, to the levels comparable to similarly treated WT cells (Figure 6H). Altogether, these data demonstrate that GILZ interacts with Smad proteins and ensures the efficient TGF-β-induced transcriptional cascade for the expression of the Treg master regulator FoxP3.

DISCUSSION

$FoxP3^+$ Treg cells are central in the control of immune and inflammatory processes. Because GCs have been shown to increase the expression of FoxP3 and the abundance of Treg cells, we addressed the possible role of GC effector GILZ in the development and function of $FoxP3^+$ Treg cells and its requirement for the GC effects on Treg cell frequency.

We have found that genetic ablation of GILZ in T cells results in a reduced number of $CD4^+FoxP3^+$ cells in the spleens, mLNs, and colon LP without affecting the number and function of mature $CD4^+$ and $CD8^+$ cells. GILZ deficiency also did not affect the number of Treg cells in the thymus, suggesting that GILZ is dispensable for the tTreg cell development. This is consistent with the notion that the TGF-β axis is mainly required for generation of pTreg but not of tTreg cells (Pesu et al., 2008; Samstein et al., 2012; Schlenner et al., 2012; Takimoto et al., 2010; Zheng et al., 2010).

Recent advances have allowed the use of Nrp-1 expression to distinguish Treg cells produced in the thymus ($FoxP3^+Nrp\text{-}1^+$) from peripherally derived pTreg cells ($FoxP3^+Nrp\text{-}1^-$), generated by conversion of mature $CD4^+$ Tconv cells (Weiss et al., 2012; Yadav et al., 2012) under steady-state conditions. The frequency and number of $FoxP3^+Nrp\text{-}1^-$ pTreg cells were reduced about 50% in the spleens and 70% in mLNs of *gilz* cKO mice, whereas the number of $FoxP3^+Nrp\text{-}1^+$ tTreg cells was unaltered, consistent with normal tTreg and defective pTreg cell formation. Indeed, the decrease in Treg cell frequency and number becomes striking in in vivo conversion experiments, strongly evidencing the defect in pTreg induction in the absence of GILZ. Lack of difference in Treg number in newborn and 3- to 8-week-old mice (data not shown) is consistent with the differences appearing with the onset of pTreg development (Yadav et al., 2012). Accordingly, the decrease in Treg cells was more evident in colon LP, a site known to support pTreg cell generation (Curotto de Lafaille and Lafaille, 2009; Yadav et al., 2013). Similarly, abrogation of Smad binding to CNS1 in mice affected the induction of pTreg cells at mucosal sites without affecting the number of Treg cells in the thymus (Josefowicz et al., 2012b; Schlenner et al., 2012; Weiss et al., 2012; Zheng et al., 2010). The fact that the pTreg production was not completely abrogated in *gilz* cKO mice suggests that other factors collaborate with GILZ in Treg cell generation. Taken together, our data demonstrate that the absence of GILZ affects the number of extrathymically generated Treg cells in several settings: number of spontaneously generated pTreg cells, through conversion in vivo from Tconv cells, and in vitro, using TGF-β.

Expression pattern of GILZ in Tconv and Treg cells supports the hypothesis that GILZ is required in naive T cells that undergo Treg differentiation in the periphery because GILZ protein is mostly detectable in $CD4^+CD25^-$ cells and not in $CD4^+CD25^+$ Treg-enriched cells. Consistently, GILZ seems to regulate the production of Treg cells and not their suppressive activity because the fewer Treg cells that are nonetheless formed without GILZ are equally potent in the suppression of T cell activation as addressed in an experimental colitis model, suggesting that GILZ is dispensable for Treg suppressive function. Similarly, collective ablation of Smad2/Smad3 or CNS1 decreases pTreg cell conversion in vivo without negatively affecting their function and maintenance (Gu et al., 2012; Josefowicz et al., 2012b).

Consistent with the lack of tTreg defect and unaltered suppressive function, *gilz* cKO mice did not display systemic autoimmunity or premature mortality associated with general Treg cell deletion (Josefowicz et al., 2012b; Kim et al., 2007). However, they develop intestinal inflammation over time, associated with an increase in IFN-γ production. Therefore, we demonstrate that, in addition to the described role of pTreg cells in the regulation of Th2-type responses at mucosal body surfaces

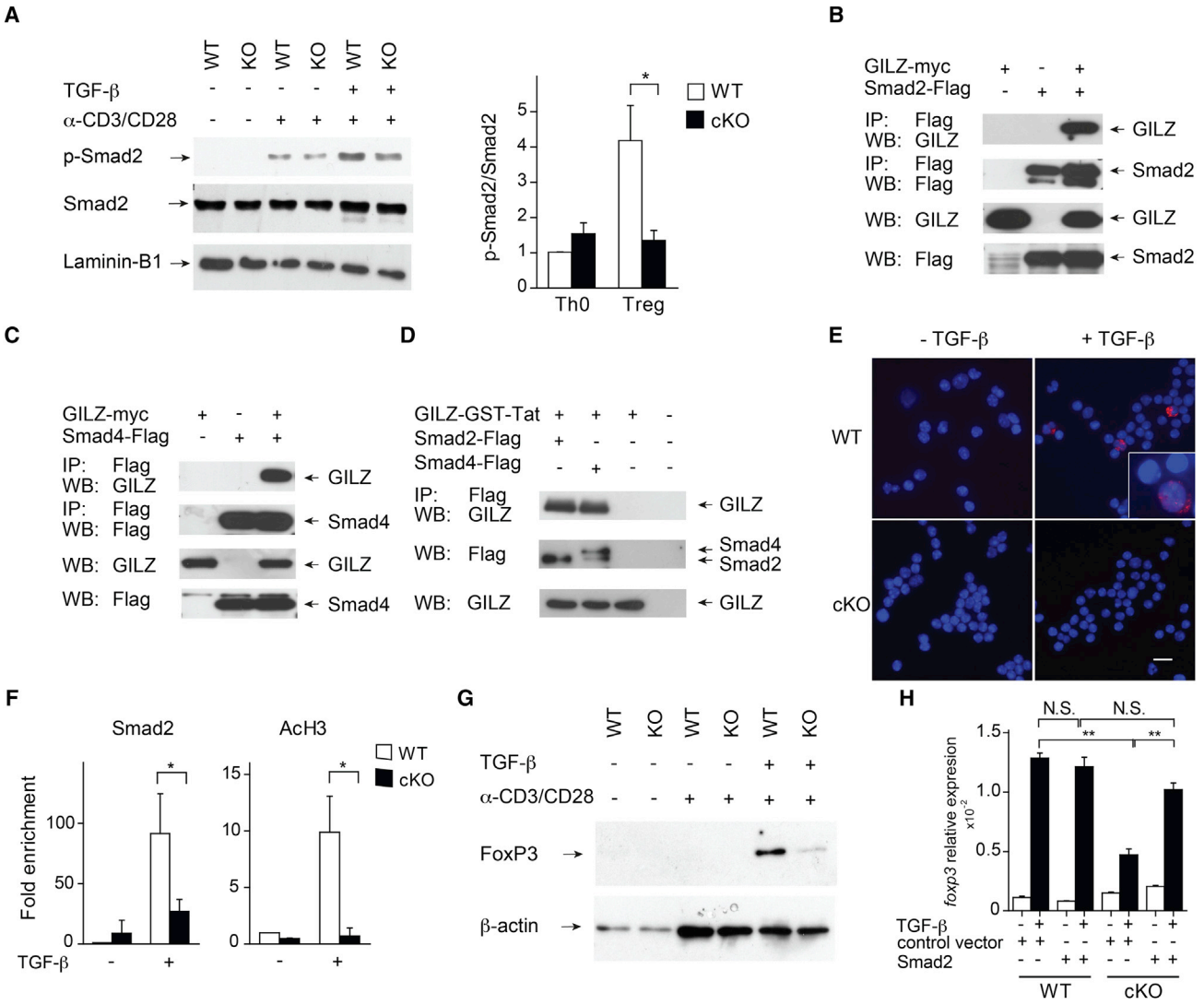

Figure 6. GILZ Enhances TGF-β Signaling and FoxP3 Expression via Direct Stimulation of TGF-β Signaling

(A) WB analysis of p-Smad2 and Smad2 in WT and *gilz* cKO $CD4^+CD25^-$ cells unstimulated or stimulated for 30 min with TGF-β in the presence of plate bound anti-CD3 and anti-CD28 Abs. Graph to the right shows densitometry analysis of the p-Smad2-to-total Smad2 ratio.

(B and C) GILZ interacts with Smad2 and Smad4 proteins in vivo. 293T cells were cotransfected with GILZ and FLAG-tagged Smad2 (B) or Smad4 (C). Immunoprecipitations (IP) were done with anti-Flag agarose beads, and the presence of GILZ (top panel) and Smads (second panel from the top) in immunoprecipitates was evaluated by WB with antibodies against GILZ, or Flag.

(D) IP-WB analysis of the direct binding between Flag-Smad2, Flag-Smad4 and GST-Tat-GILZ purified from bacterial extracts.

(E) GILZ-Smad2 interaction in native T cells. Immunofluorescence images of in situ PLA performed on $CD4^+CD25^-$ T cells isolated from WT and *gilz* cKO mice and activated in vitro for 30 min with plate bound anti-CD3 and anti-CD28 Abs, without (left panels) or with 5 ng/ml TGF-β (right panels). PLA was performed using GILZ/Smad2 antibody mix. A representative merge of the red (PLA) and blue (DAPI) channel images is shown for each sample. Scale bar, 50 μm.

(F) ChIP assay of Smad2 binding and histone acetylation at the *foxp3* CNS1 in WT and *gilz* cKO splenic $CD4^+CD25^-$ T cells stimulated for 30 min (for Smad2) and 24 hr (for AcH3) as in (A). Cell lysates were immunoprecipitated with anti-Smad2 (left), anti-acetyl histone 3 (AcH3), or control IgG, and the presence of specific regions in the immunoprecipitates was determined by quantitative real-time PCR.

(G) WB analysis of FoxP3 expression in WT and *gilz* cKO splenic $CD4^+CD25^-$ cells stimulated for 48 hr as in (A). An equal number of cells was loaded, and β-actin protein expression was used as a loading control.

(H) Expression of *foxp3* mRNA in WT and *gilz* cKO $CD4^+CD25^-$ T cells stimulated as in (A) for 24 hr, following the cell nucleofection with Smad2-expressing or control vectors.

Graphs represent mean ± SEM of data pooled from two (F and H) or three (A) experiments. See also Figure S6.

(Josefowicz et al., 2012b), the reduction of pTreg cells in *gilz* cKO mice results in an increased susceptibility to Th1-type intestinal inflammation.

Treg cells are critical in controlling intestinal immune homeostasis. In colon, ablation of Treg cells leads to lethal intestinal inflammation during experimentally induced colitis (Boehm

et al., 2012), whereas Treg reduction is observed in IBD (Eastaff-Leung et al., 2010). pTreg cells are generated and abundant in colon LP and are essential to control colitis. Importantly, treatment with Treg cells resolved the colitis in an adoptive transfer model, but only when pTreg cells were also present, further stressing the potential distinct specialized function for pTreg cells (Haribhai et al., 2009). An increase of colonic Treg cell number induced by microbiota and its derivatives was shown to correlate with suppression of the disease symptoms in an experimental colitis model (Atarashi et al., 2011; Smith et al., 2013). Consistently, mice with GILZ overexpression in T cells show resistance to chemically induced colitis (Cannarile et al., 2009; Delfino et al., 2004). Our data show that these mice contain numerically more Treg cells in the periphery, which could improve immune tolerance in these mice. Accordingly, a numeric decrease in pTreg cells in *gilz* cKO mice is associated with an increased susceptibility to DNBS-induced Th1-type colitis, a phenotype that is reverted by the transfer of Treg cells. Therefore, the colitis susceptibility correlates with the Treg cell number changes, and not with the enhanced production of IFN-γ, IL-4, and IL-17 cytokines. Although the effect of GILZ deficiency on Teff cell function cannot be excluded, as suggested by Th1 skewing, our data suggest that the numeric reduction in pTreg cells in the absence of apparent functional differences in Teff cells results in an increased susceptibility to colitis. Such results have potential clinical implications because monitoring and restoring adequate Treg levels may be exploited to cure IBD and other autoimmune diseases.

Notably, *gilz* cKO mice were resistant to the therapeutic action of GCs, which reduced the clinical features of colitis, such body weight loss, diarrhea, and colon shortening in mice only if GILZ was present. GC treatment led to the increase in the Treg/Teff ratio in WT but not in GILZ-deficient mice. Both in mice with ongoing colitis and in unmanipulated mice, the frequency of $CD4^+FoxP3^+$ cells increases upon treatment with Dex dependent on GILZ, thus demonstrating that GILZ mediates the events triggered by Dex in T cells that lead to an increase in Treg number. Importantly, we demonstrated that GCs promoted TGF-β-induced FoxP3 expression in GILZ-sufficient but not in GILZ-deficient cells, suggesting that GC and TGF-β cooperation requires the action of GILZ.

We found that GILZ regulates TGF-β signaling. Duration and strength of TGF-β signaling depend on Smad transcriptional activity, which can be regulated at multiple levels, including TGF-β receptor activity, interactions with nuclear binding partners, and nuclear phosphatase activity (Li and Flavell, 2008). It has been shown that both Smad2 and Smad3 contribute to TGF-β-mediated *foxp3* induction (Nolting et al., 2009; Takimoto et al., 2010; Tone et al., 2008; Xu et al., 2010). Interestingly, GILZ interacts with both Smad2 (receptor activated) and Smad4 (cytoplasmic/nuclear), but not Smad3. Importantly, interaction of the endogenous GILZ and Smad2 was detected also in TGF-β-stimulated native T cells. In the absence of GILZ, TGF-β-dependent p-Smad2 is reduced, so as its consequent binding to the CNS1 region and expression of FoxP3. Similar to retinoic acid, GCs may facilitate the access of transcription factors such as Smads to *foxp3* locus via induction of GILZ (Nolting et al., 2009; Xu et al., 2010).

Therefore, in addition to retinoic acid, microbiota, and its metabolites (Atarashi et al., 2011; Coombes et al., 2007; Smith et al., 2013; Sun et al., 2007), GILZ appears to contribute to the TGF-β-mediated generation of the pTreg cells and control intestinal homeostasis. Interestingly, colonic epithelial cells produce GCs locally at steady state and during inflammation (Cima et al., 2004). Thus, strategies involving modulation of GILZ expression might prove useful to enhance peripheral tolerance.

Altogether, these data establish GILZ as a modulator of Treg cell homeostasis and suggest a physiologic crosstalk between TGF-β signaling and stress hormones. Our study suggests that the loss of pTreg cells in disease can be controlled with GCs or with novel strategies involving GILZ. Besides clinical aspects, our work opens new perspectives for the potential role of stress hormones in physiologic modulation of Treg-controlled processes including suppression of protective and damaging immune responses.

EXPERIMENTAL PROCEDURES

Mice

Mice bearing a floxed *gilz* allele were generated and maintained on a C57Bl/6 background as described (Bruscoli et al., 2012). CD4-Cre transgenic and $Rag1^{-/-}$ mice were purchased from Jackson Laboratory; CD45.1 mice were purchased from Charles River Laboratories. All procedures were approved by the Ethical Committee of the University of Perugia.

Antibodies and Flow Cytometry

For the list of monoclonal antibodies (mAbs) used for flow cytometry analyses, cell sorting, and in vitro assays, see Supplemental Experimental Procedures. Staining for FoxP3 was performed using the FoxP3/Transcription Factor Staining Buffer Set (eBioscience). Analysis and cell sorting were done using a one- and two-laser standard configuration FACSCanto and FACSAria II (BD Biosciences); data were analyzed using FlowJo software (TreeStar).

Adoptive Transfer of Colitis

$CD4^+CD25^+$ and naive $CD4^+CD25^-CD45Rb^{hi}$ T cells were purified from spleens by cell sorting (purity routinely exceeded 98%). A total of 400,000 $CD4^+CD25^-CD45Rb^{hi}$ T cells alone or along with 125,000 $CD4^+CD25^+$ T cells were injected intraperitoneally (i.p.) into $Rag1^{-/-}$ mice. Clinical evidence of disease and body weight were monitored weekly.

Induction of Colitis with DNBS

Mice were anesthetized with sodium thiopental (30 mg/kg) and xylazine (10 mg/kg). A total of 3 mg of DNBS or 50% ethanol (2,4-dinitrobenzenesulfonic acid; Sigma-Aldrich) was administered per rectum. Body weight, stool consistency, and rectal bleeding were examined daily, and total clinical score was calculated as in Cannarile et al. (2009). For Treg transfer experiments, 3×10^6 $CD4^+CD25^+$ cells purified by magnetic sorting from spleens and mLNs of WT mice were injected i.v. into WT or *gilz* cKO mice 1 day before DNBS administration.

In Vivo Treatment with Dex

Mice were i.p. injected with 1.5 mg/kg of Dex or PBS and then were administered with DNBS. Dex was also injected i.p. at day 1 and day 2 after DNBS administration. For studies of the Dex effect on Treg cells without induction of colitis, mice were i.p. injected with 1 mg/kg of Dex or PBS for 3 consecutive days.

Histology

Tissues were fixed overnight in 10% formalin solution (Sigma-Aldrich), dehydrated in graded ethanol, embedded in paraffin (Sigma-Aldrich), and sectioned. Sections were stained with hematoxylin and eosin (H&E) and

observed under an Olympus BX51 microscope equipped with a Leica EC3 camera.

Protein Interaction Assays and Immunoblotting

Protein extracts were obtained using RIPA buffer supplemented with protease (Sigma-Aldrich) and phosphatase (Thermo Scientific) inhibitor cocktails. Western blot (WB) analyses were performed with antibody against GILZ (eBioscience), phospho-Smad2 (Cell Signaling Technology), Smad2 (Cell Signaling Technology), FoxP3 (eBioscience), Laminin B1 (Abcam), β-actin (Sigma-Aldrich), Flag (Sigma-Aldrich), and HA (Santa Cruz Biotechnology). Coimmunoprecipitation studies were performed as described (Bereshchenko et al., 2002) using pRKW2-Smad2-Flag, pRKW2-Smad4-Flag, pcDNA3.1(+)/myc-HisB-GILZ, and pcDNA 3.1D/V5-His TOPO-Gilz-Flag expression vectors. For the direct interaction assay, One Shot BL21(DE3)pLysS (Invitrogen) bacteria were transformed with Smad2-Flag, Smad4-Flag, and GST-Tat-GILZ expression vectors, and protein-protein interaction was assayed as described by Bereshchenko et al., (2002).

In Situ Proximity Ligation Assay for Protein-Protein Interactions

Duolink proximity ligation assay (PLA) was performed according to the manufacturer's instructions (Olink Bioscience; see also Supplemental Experimental Procedures). Detection of the interaction signals was carried out by fluorescence microscopy using a Zeiss Axioplan fluorescence microscope equipped with a Spot-2 cooled camera (Diagnostic Instruments).

ChIP Assay

ChIP assays were performed as described by Tone et al. (2008). In brief, cells were fixed in 1% paraformaldehyde and sonicated on ice. Precleared lysates were incubated overnight at 4C° with polyclonal anti-Smad2 (Cell Signaling Technology), anti-acetyl histone H3 (Millipore), or control rabbit IgG (Cell Signaling Technology). Immunocomplexes were collected using the Chip Assay Kit (Millipore), and quantitative real-time PCR analysis was performed using the Power SYBR Green PCR Master Mix (Applied Biosystems) to determine the percentage of each analyzed region against input DNA. The quantitative real-time PCR primers are listed in the Supplemental Information.

Statistical Analysis

Statistical analysis was performed with Prism 6.0 (GraphPad Software). The nonparametric Mann-Whitney U test or a two-tailed unpaired Student's t test was used for statistical comparisons (*$p < 0.05$; **$p < 0.005$; ***$p < 0.0005$).

SUPPLEMENTAL INFORMATION

Supplemental Information includes Supplemental Experimental Procedures and six figures and can be found with this article online at http://dx.doi.org/10.1016/j.celrep.2014.03.004.

ACKNOWLEDGMENTS

This work was supported by Associazione Italiana per la Ricerca sul Cancro (IG-10677 and IG-14291 to C.R.). O.B. was a recipient of the José Carreras/EHA Young Investigator Award. We thank E. Bonifacio and E.D. Bilbao for expert assistance in cell sorting, S. Ronchetti for assisting with PLA experiments, G. Darrasse-Jèze for advice on the Treg maintenance experiments and critical reading of the manuscript, and R. Dalla-Favera for helpful discussions and critical reading of the manuscript.

Received: October 17, 2013
Revised: January 30, 2014
Accepted: March 3, 2014
Published: April 3, 2014

REFERENCES

Atarashi, K., Tanoue, T., Shima, T., Imaoka, A., Kuwahara, T., Momose, Y., Cheng, G., Yamasaki, S., Saito, T., Ohba, Y., et al. (2011). Induction of colonic regulatory T cells by indigenous Clostridium species. Science *331*, 337–341.

Ayroldi, E., Migliorati, G., Bruscoli, S., Marchetti, C., Zollo, O., Cannarile, L., D'Adamio, F., and Riccardi, C. (2001). Modulation of T-cell activation by the glucocorticoid-induced leucine zipper factor via inhibition of nuclear factor kappaB. Blood *98*, 743–753.

Barrat, F.J., Cua, D.J., Boonstra, A., Richards, D.F., Crain, C., Savelkoul, H.F., de Waal-Malefyt, R., Coffman, R.L., Hawrylowicz, C.M., and O'Garra, A. (2002). In vitro generation of interleukin 10-producing regulatory CD4(+) T cells is induced by immunosuppressive drugs and inhibited by T helper type 1 (Th1)- and Th2-inducing cytokines. J. Exp. Med. *195*, 603–616.

Bereshchenko, O.R., Gu, W., and Dalla-Favera, R. (2002). Acetylation inactivates the transcriptional repressor BCL6. Nat. Genet. *32*, 606–613.

Boehm, F., Martin, M., Kesselring, R., Schiechl, G., Geissler, E.K., Schlitt, H.J., and Fichtner-Feigl, S. (2012). Deletion of Foxp3+ regulatory T cells in genetically targeted mice supports development of intestinal inflammation. BMC Gastroenterol. *12*, 97.

Bruscoli, S., Donato, V., Velardi, E., Di Sante, M., Migliorati, G., Donato, R., and Riccardi, C. (2010). Glucocorticoid-induced leucine zipper (GILZ) and long GILZ inhibit myogenic differentiation and mediate anti-myogenic effects of glucocorticoids. J. Biol. Chem. *285*, 10385–10396.

Bruscoli, S., Velardi, E., Di Sante, M., Bereshchenko, O., Venanzi, A., Coppo, M., Berno, V., Mameli, M.G., Colella, R., Cavaliere, A., and Riccardi, C. (2012). Long glucocorticoid-induced leucine zipper (L-GILZ) protein interacts with ras protein pathway and contributes to spermatogenesis control. J. Biol. Chem. *287*, 1242–1251.

Cannarile, L., Fallarino, F., Agostini, M., Cuzzocrea, S., Mazzon, E., Vacca, C., Genovese, T., Migliorati, G., Ayroldi, E., and Riccardi, C. (2006). Increased GILZ expression in transgenic mice up-regulates Th-2 lymphokines. Blood *107*, 1039–1047.

Cannarile, L., Cuzzocrea, S., Santucci, L., Agostini, M., Mazzon, E., Esposito, E., Muià, C., Coppo, M., Di Paola, R., and Riccardi, C. (2009). Glucocorticoid-induced leucine zipper is protective in Th1-mediated models of colitis. Gastroenterology *136*, 530–541.

Chen, X., Murakami, T., Oppenheim, J.J., and Howard, O.M. (2004). Differential response of murine CD4+CD25+ and CD4+CD25- T cells to dexamethasone-induced cell death. Eur. J. Immunol. *34*, 859–869.

Chen, X., Oppenheim, J.J., Winkler-Pickett, R.T., Ortaldo, J.R., and Howard, O.M. (2006). Glucocorticoid amplifies IL-2-dependent expansion of functional FoxP3(+)CD4(+)CD25(+) T regulatory cells in vivo and enhances their capacity to suppress EAE. Eur. J. Immunol. *36*, 2139–2149.

Chung, I.Y., Dong, H.F., Zhang, X., Hassanein, N.M., Howard, O.M., Oppenheim, J.J., and Chen, X. (2004). Effects of IL-7 and dexamethasone: induction of CD25, the high affinity IL-2 receptor, on human CD4+ cells. Cell. Immunol. *232*, 57–63.

Cima, I., Corazza, N., Dick, B., Fuhrer, A., Herren, S., Jakob, S., Ayuni, E., Mueller, C., and Brunner, T. (2004). Intestinal epithelial cells synthesize glucocorticoids and regulate T cell activation. J. Exp. Med. *200*, 1635–1646.

Coombes, J.L., Siddiqui, K.R., Arancibia-Cárcamo, C.V., Hall, J., Sun, C.M., Belkaid, Y., and Powrie, F. (2007). A functionally specialized population of mucosal CD103+ DCs induces Foxp3+ regulatory T cells via a TGF-beta and retinoic acid-dependent mechanism. J. Exp. Med. *204*, 1757–1764.

Curotto de Lafaille, M.A., and Lafaille, J.J. (2009). Natural and adaptive foxp3+ regulatory T cells: more of the same or a division of labor? Immunity *30*, 626–635.

D'Adamio, F., Zollo, O., Moraca, R., Ayroldi, E., Bruscoli, S., Bartoli, A., Cannarile, L., Migliorati, G., and Riccardi, C. (1997). A new dexamethasone-induced gene of the leucine zipper family protects T lymphocytes from TCR/CD3-activated cell death. Immunity *7*, 803–812.

Delfino, D.V., Agostini, M., Spinicelli, S., Vito, P., and Riccardi, C. (2004). Decrease of Bcl-xL and augmentation of thymocyte apoptosis in GILZ overexpressing transgenic mice. Blood *104*, 4134–4141.

Eastaff-Leung, N., Mabarrack, N., Barbour, A., Cummins, A., and Barry, S. (2010). Foxp3+ regulatory T cells, Th17 effector cells, and cytokine environment in inflammatory bowel disease. J. Clin. Immunol. *30*, 80–89.

Faubion, W.A., Jr., Loftus, E.V., Jr., Harmsen, W.S., Zinsmeister, A.R., and Sandborn, W.J. (2001). The natural history of corticosteroid therapy for inflammatory bowel disease: a population-based study. Gastroenterology *121*, 255–260.

Feuerer, M., Hill, J.A., Mathis, D., and Benoist, C. (2009). Foxp3+ regulatory T cells: differentiation, specification, subphenotypes. Nat. Immunol. *10*, 689–695.

Fisson, S., Darrasse-Jèze, G., Litvinova, E., Septier, F., Klatzmann, D., Liblau, R., and Salomon, B.L. (2003). Continuous activation of autoreactive CD4+ CD25+ regulatory T cells in the steady state. J. Exp. Med. *198*, 737–746.

Gu, A.D., Wang, Y., Lin, L., Zhang, S.S., and Wan, Y.Y. (2012). Requirements of transcription factor Smad-dependent and -independent TGF-β signaling to control discrete T-cell functions. Proc. Natl. Acad. Sci. USA *109*, 905–910.

Haribhai, D., Lin, W., Edwards, B., Ziegelbauer, J., Salzman, N.H., Carlson, M.R., Li, S.H., Simpson, P.M., Chatila, T.A., and Williams, C.B. (2009). A central role for induced regulatory T cells in tolerance induction in experimental colitis. J. Immunol. *182*, 3461–3468.

Haribhai, D., Williams, J.B., Jia, S., Nickerson, D., Schmitt, E.G., Edwards, B., Ziegelbauer, J., Yassai, M., Li, S.H., Relland, L.M., et al. (2011). A requisite role for induced regulatory T cells in tolerance based on expanding antigen receptor diversity. Immunity *35*, 109–122.

Hu, Y., Tian, W., Zhang, L.L., Liu, H., Yin, G.P., He, B.S., and Mao, X.M. (2012). Function of regulatory T-cells improved by dexamethasone in Graves' disease. Eur. J. Endocrinol. *166*, 641–646.

Josefowicz, S.Z., Lu, L.F., and Rudensky, A.Y. (2012a). Regulatory T cells: mechanisms of differentiation and function. Annu. Rev. Immunol. *30*, 531–564.

Josefowicz, S.Z., Niec, R.E., Kim, H.Y., Treuting, P., Chinen, T., Zheng, Y., Umetsu, D.T., and Rudensky, A.Y. (2012b). Extrathymically generated regulatory T cells control mucosal TH2 inflammation. Nature *482*, 395–399.

Kadmiel, M., and Cidlowski, J.A. (2013). Glucocorticoid receptor signaling in health and disease. Trends Pharmacol. Sci. *34*, 518–530.

Karagiannidis, C., Akdis, M., Holopainen, P., Woolley, N.J., Hense, G., Rückert, B., Mantel, P.Y., Menz, G., Akdis, C.A., Blaser, K., and Schmidt-Weber, C.B. (2004). Glucocorticoids upregulate FOXP3 expression and regulatory T cells in asthma. J. Allergy Clin. Immunol. *114*, 1425–1433.

Kim, J.M., Rasmussen, J.P., and Rudensky, A.Y. (2007). Regulatory T cells prevent catastrophic autoimmunity throughout the lifespan of mice. Nat. Immunol. *8*, 191–197.

Li, M.O., and Flavell, R.A. (2008). TGF-beta: a master of all T cell trades. Cell *134*, 392–404.

Ling, Y., Cao, X., Yu, Z., and Ruan, C. (2007). Circulating dendritic cells subsets and CD4+Foxp3+ regulatory T cells in adult patients with chronic ITP before and after treatment with high-dose dexamethasome. Eur. J. Haematol. *79*, 310–316.

Nolting, J., Daniel, C., Reuter, S., Stuelten, C., Li, P., Sucov, H., Kim, B.G., Letterio, J.J., Kretschmer, K., Kim, H.J., and von Boehmer, H. (2009). Retinoic acid can enhance conversion of naive into regulatory T cells independently of secreted cytokines. J. Exp. Med. *206*, 2131–2139.

Pesu, M., Watford, W.T., Wei, L., Xu, L., Fuss, I., Strober, W., Andersson, J., Shevach, E.M., Quezado, M., Bouladoux, N., et al. (2008). T-cell-expressed proprotein convertase furin is essential for maintenance of peripheral immune tolerance. Nature *455*, 246–250.

Powrie, F., Leach, M.W., Mauze, S., Caddle, L.B., and Coffman, R.L. (1993). Phenotypically distinct subsets of CD4+ T cells induce or protect from chronic intestinal inflammation in C. B-17 scid mice. Int. Immunol. *5*, 1461–1471.

Prado, C., Gómez, J., López, P., de Paz, B., Gutiérrez, C., and Suárez, A. (2011). Dexamethasone upregulates FOXP3 expression without increasing regulatory activity. Immunobiology *216*, 386–392.

Samstein, R.M., Josefowicz, S.Z., Arvey, A., Treuting, P.M., and Rudensky, A.Y. (2012). Extrathymic generation of regulatory T cells in placental mammals mitigates maternal-fetal conflict. Cell *150*, 29–38.

Schlenner, S.M., Weigmann, B., Ruan, Q., Chen, Y., and von Boehmer, H. (2012). Smad3 binding to the foxp3 enhancer is dispensable for the development of regulatory T cells with the exception of the gut. J. Exp. Med. *209*, 1529–1535.

Smith, P.M., Howitt, M.R., Panikov, N., Michaud, M., Gallini, C.A., Bohlooly-Y, M., Glickman, J.N., and Garrett, W.S. (2013). The microbial metabolites, short-chain fatty acids, regulate colonic Treg cell homeostasis. Science *341*, 569–573.

Suárez, A., López, P., Gómez, J., and Gutiérrez, C. (2006). Enrichment of CD4+ CD25high T cell population in patients with systemic lupus erythematosus treated with glucocorticoids. Ann. Rheum. Dis. *65*, 1512–1517.

Sun, C.M., Hall, J.A., Blank, R.B., Bouladoux, N., Oukka, M., Mora, J.R., and Belkaid, Y. (2007). Small intestine lamina propria dendritic cells promote de novo generation of Foxp3 T reg cells via retinoic acid. J. Exp. Med. *204*, 1775–1785.

Takimoto, T., Wakabayashi, Y., Sekiya, T., Inoue, N., Morita, R., Ichiyama, K., Takahashi, R., Asakawa, M., Muto, G., Mori, T., et al. (2010). Smad2 and Smad3 are redundantly essential for the TGF-beta-mediated regulation of regulatory T plasticity and Th1 development. J. Immunol. *185*, 842–855.

Tone, Y., Furuuchi, K., Kojima, Y., Tykocinski, M.L., Greene, M.I., and Tone, M. (2008). Smad3 and NFAT cooperate to induce Foxp3 expression through its enhancer. Nat. Immunol. *9*, 194–202.

Weiss, J.M., Bilate, A.M., Gobert, M., Ding, Y., Curotto de Lafaille, M.A., Parkhurst, C.N., Xiong, H., Dolpady, J., Frey, A.B., Ruocco, M.G., et al. (2012). Neuropilin 1 is expressed on thymus-derived natural regulatory T cells, but not mucosa-generated induced Foxp3+ T reg cells. J. Exp. Med. *209*, 1723–1742.

Xu, L., Kitani, A., Stuelten, C., McGrady, G., Fuss, I., and Strober, W. (2010). Positive and negative transcriptional regulation of the Foxp3 gene is mediated by access and binding of the Smad3 protein to enhancer I. Immunity *33*, 313–325.

Yadav, M., Louvet, C., Davini, D., Gardner, J.M., Martinez-Llordella, M., Bailey-Bucktrout, S., Anthony, B.A., Sverdrup, F.M., Head, R., Kuster, D.J., et al. (2012). Neuropilin-1 distinguishes natural and inducible regulatory T cells among regulatory T cell subsets in vivo. J. Exp. Med. *209*, 1713–1722.

Yadav, M., Stephan, S., and Bluestone, J.A. (2013). Peripherally induced tregs - role in immune homeostasis and autoimmunity. Frontiers in immunology *4*, 232.

Yosef, N., Shalek, A.K., Gaublomme, J.T., Jin, H., Lee, Y., Awasthi, A., Wu, C., Karwacz, K., Xiao, S., Jorgolli, M., et al. (2013). Dynamic regulatory network controlling TH17 cell differentiation. Nature *496*, 461–468.

Zheng, Y., Josefowicz, S., Chaudhry, A., Peng, X.P., Forbush, K., and Rudensky, A.Y. (2010). Role of conserved non-coding DNA elements in the Foxp3 gene in regulatory T-cell fate. Nature *463*, 808–812.